

# Positioning value of objective analysis of macular ganglion cell complex (mGCC) in optic pathway-related neuro-ophthalmology

Wei Zhang

Beijing Tongren Hospital <https://orcid.org/0000-0002-7527-2217>

Xin-quan Sun

China-Japan Friendship Hospital

Xiao-yan Peng (✉ [drzhangwei2014@163.com](mailto:drzhangwei2014@163.com))

---

## Research article

**Keywords:** macular ganglion cell complex (mGCC), Neuro-ophthalmology, swept-source optical coherence tomography (SS-OCT)

**Posted Date:** December 13th, 2019

**DOI:** <https://doi.org/10.21203/rs.2.13517/v2>

**License:** © ⓘ This work is licensed under a Creative Commons Attribution 4.0 International License.

[Read Full License](#)

---

# Abstract

## Objective

This study aimed to explore the positioning value of objective analysis of macular ganglion cell complex (mGCC) in optic pathway-related neuro-ophthalmology diseases.

## Methods

In this retrospective case study, a total of 32 patients with optic pathway-related neuro-ophthalmology diseases were enrolled. A swept-source optical coherence tomography (SS-OCT) was used to scan and analyze the morphological characteristics of the mGCC thickness and the peripapillary retinal nerve fiber layer (pRNFL) thickness in these patients, which were compared with the vision changes at the corresponding phase to analyze their relationship.

## Results

In optic pathway-related neuro-ophthalmologic diseases, the morphological characteristics of mGCC thickness demonstrated characteristic changes that are similar to that of vision, and mGCC analysis remained to be objective.

## Conclusion

The application of SS-OCT to examine the morphological changes of mGCC thickness has the value of objective positioning analysis in the diagnosis and treatment of optic pathway-related neuro-ophthalmologic diseases.

# Background

With the development of ophthalmic diagnostic techniques, swept-source optical coherence tomography (SS-OCT) is widely used in the diagnosis and treatment of neuro-ophthalmologic diseases due to its rapid process, high-resolution and non-invasiveness.<sup>1-3</sup> This technique in turn provides favorable conditions for observing the retinal ganglion cells in the optic nerve and macular area.<sup>4,5</sup> Most of the previous OCT studies focused on observing the thickness of the optic nerve fiber layer present around the optic disc and the thickness of the retinal ganglion cells in the macular area,<sup>6-9</sup> while there is a lack of studies describing the morphological characteristics of the ganglion cells in the macular area. Hence, in the present study, SS-OCT was used to examine the topographical map of macular ganglion cell complex (mGCC) thickness and the topographic map of the nerve fiber thickness around the optic disc. The probability of the changes in mGCC atrophy and thinning pattern combined with visual field examination were adopted to analyze the changes in imaging the optic pathway-related neuro-ophthalmologic diseases. We aimed to observe the changes in the optic nerve of the above diseases from a new imaging perspective, thereby deepen the understanding of the pathological and physiological changes of these diseases.

## Methods

General data: Thirty-two patients with optic pathway-related neuro-ophthalmology diseases who visited our ophthalmology center were collected (Table 1), which included 15 males and 17 females, aged 5–77 years, and with visual range 20/800–20/16. Among them, 12 cases had pituitary tumors, 3 had craniopharyngioma, 2 had transparent septum deficiency, 3 had hemangioma, 2 had vascular malformation, 6 had ischemia, 1 had meningioma, 1 had schwannoma, 1 had chordoma or metastatic carcinoma and 1 had other tumors.

### Methods

Routine examinations including distance vision, near vision, intraocular pressure, slit lamp microscope, and mydriasis funduscopy were performed. In terms of perimetric examination, an automatic visual field analyzer was used for central 30°, 60° and 90° examinations.

SS-OCT examination and image analysis: SS-OCT was used to analyze the morphological features in mGCC thickness map, and the peripapillary retinal nerve fiber layer (pRNFL) thickness as well as its clinically significant probability of the lesions. These were compared with the visual field changes at the corresponding phase, thereby analyzing their relationship.

## Results

The visual field, mGCC atrophy and lesion positioning of the 32 patients with optic pathway-related neuro-ophthalmology mainly showed (1) upper visual field hemianopia based on monocular horizontal demarcation, mGCC was manifested as lower atrophy, and the lesion could be diagnosed as optic neuropathy at the anterior lamina cribrosa (for cases 31 and 32). In case of monocular complete blindness, the mGCC was manifested as complete atrophy, and the lesion could be considered as optic neuropathy from posterior lamina cribrosa to anterior optic chiasm (such as unilateral retrobulbar optic neuritis, optic canal fracture). (2) For bitemporal hemianopia, the bilateral mGCC rings showed nasal atrophy by taking midperpendicular bisector as demarcation, and the lesion was located at the optic chiasm (such as in cases 1, 2, 6, 7, 18, 22, and 23). In terms of bitemporal hemianopia and one eye crossing the midperpendicular bisector, the bilateral mGCC rings were manifested as nasal atrophy by taking the midperpendicular bisector as demarcation and one eye crossed the midperpendicular bisector, and the lesion was considered as optic chiasm lesion biased towards one eye (such as in cases 4, 5, 8, 19, 20, 21, 24, 26, and 28). (3) For homonymous hemianopia without macular sparing, mGCC was manifested as nasal atrophy in one eye and temporal atrophy in another eye by taking the midperpendicular bisector as demarcation, and the patients were diagnosed as lesion from the posterior optic chiasm till before the middle of the optic radiation (such as in cases 3, 9, 14 and 25). For cases with both eyes of hemianopia towards 1/4 upper or lower quadrant, without the macula sparing, the mGCC ring was manifested as atrophy at 1/4 of the lower nasal side in one eye and atrophy at 1/4 of the lower temporal side in the other eye, and the lesion was located at the anterior optic radiation (such as in case

12). In terms of homonymous hemianopia with macular sparing, mGCC was manifested as nasal atrophy in one eye and temporal atrophy in another eye by taking the midperpendicular bisector as demarcation, and the lesion was located at the posterior optic radiation and further (such as in cases 10, 13, 15). For homonymous hemianopia with macular sparing and retain of contralateral 30-degree crescent, mGCC was manifested as nasal atrophy in one eye and temporal atrophy in another eye by taking the midperpendicular bisector as demarcation, with macular sparing, and the lesion was located in the middle of the calcarine fissure (such as in case 17). If the visual field was symmetric and ipsilateral central hemianopia, mGCC appeared as nasal atrophy in one eye and temporal atrophy in another eye by taking the midperpendicular bisector as demarcation, with macular sparing, and the lesion was positioned at the occipital pole. Meanwhile, if the visual field was symmetric and ipsilateral hemianopia, with the meniscal defects at the contralateral eye, the mGCC appeared as nasal atrophy in one eye and temporal atrophy in another eye by taking the midperpendicular bisector as demarcation, with macular sparing, and the lesion was positioned at the anterior calcarine fissure. (4) Altered visual field and normal mGCC ring were found in patients with short onset time, either in the latent period or early onset (such as in cases 27, 29, and 30), and with descending optic neuropathy of trans-neuronal lesion after optic radiation that had not induced mGCC injury, wherein the lesion positioning was relied on the visual field and MRI (such as in cases 11 and 16), (Figure 1).

## Discussion

Optic pathway-related neuro-ophthalmologic diseases mainly included optic nerve, optic chiasm, optic tract, optic radiation, inflammation of the central nervous system, tumor, trauma, degeneration and congenital dysplasia and other diseases. Ganglion cell complex-optic nerve is the pivotal pathway that connects the retina and the brain.<sup>10</sup> The nerve conduction begins in the ganglion cell complex (dendrites-inner plexiform layer, ganglion cell layer, axon-neural fiber layer) and nerve fiber bundle, converging at the lamina cribrosa till the optic nerve. The bilateral optic nerves form optic chiasm in the suprasellar region, and then divide into bilateral optic tracts, exchanging the neurons at the lateral geniculate nucleus (LGN). These in turn form optic radiation that projects towards the fissura calcarina, and finally the visual information is completed by the visual center in the occipital region. As the optic nerve fibers travel in clear regularity, the nasal retinal nerve fibers (including the nasal part of the macula) of each eye intersect at the optic chiasm till the contralateral tract, while those at the temporal side do not intersect.<sup>11</sup> The inferior retinal nerve fibers are located in the medial optic tract after passing through the optic nerve and the optic chiasm. Hence, the optic nerve fibers rotate 90° when they enter the optic tract from the optic nerve and the optic chiasm. The subnasal retinal nerve fibers pass through the optic chiasm, but travel forward in the contralateral optic nerve (Wilbrand's knee) before merging with contralateral inferotemporal non-crossing-fibers and entering the optic tract.<sup>12</sup> Therefore, the diseases at different parts of optic pathway-related neuro-ophthalmology have regularity, and manifest as visual field changes with different regularities. Meanwhile, the visual field examination is subjective, and is largely influenced by the visual function, psychological factors and cognitive coordination ability of the patients. The macular region accounts for 50% of ganglion cells, and are arranged regularly.<sup>13-15</sup> The normal mGCC

manifests as a ring structure, which is a yellow ring, while the mGCC in subnormal status or in the swelling period was manifested as a red ring. The common atrophic forms of mGCC included: 1/4 quadrant atrophy, upper and lower atrophy based on horizontal demarcation, binasal or concurrent homonymous atrophy or complete atrophy by taking the midperpendicular bisector as demarcation (Figure 2).

Through clinical diagnosis and treatment, we found that the ganglion cells were distributed in the macular region also and were presented in precise horizontal, vertical and quadrant regularity. Specifically, they manifest as unilateral mGCC ring atrophy and thinning or mGCC atrophy at the upper and lower half side based on horizontal demarcation for the lesion at anterior optic chiasm, the mGCC atrophy and thinning at half of the bilateral nasal sides based on midperpendicular demarcation for the lesion at optic chiasm, and the mGCC atrophy with or without macular sparing at homonymous side or 1/4 quadrant based on midperpendicular demarcation for lesion at posterior optic chiasm. The combination of MRI and 90-degree field of view should be performed to analyze the accurate positioning of the visual pathological lesions at the posterior optic chiasm. The results showed that the visual tract lesions as well as lesions at the anterior and the middle of the optic tract were not accompanied by macular sparing, while the lesions at the posterior optic radiation and the subsequent calcarine fissure were accompanied by macular sparing. The mGCC showed atrophy and thinning at 1/4 quadrant below the same name for lesions at the anterior ring of optic radiation, while showed atrophy and thinning at 1/4 quadrant above the same name for lesions in present in the medial optic radiation. In calcarine fissure lesions, the mGCC showed semi-asymmetric atrophy in the same name with macular sparing based on midperpendicular demarcation, while appeared symmetric ipsilateral hemianopia under 90-degree field of view for lesions in the middle of calcarine fissure, with macular sparing and contralateral crescent sparing. The mGCC showed a crescent defect in the contralateral eye under the 90-degree field of view for lesions in anterior calcarine fissure, while manifested as symmetric and ipsilateral central hemianopia (Figure 3) under 90-degree field of view for lesions at the occipital pole.

The visual field of pre-beam disease, the mGCC and the pRNFL damage evolution are divided into three stages: (1) Subnormal eyes at the preclinical or latent period showed normal vision and field of view, with mGCC and pRNFL swelling. (2) Subnormal eyes at the beginning of the disease lasted for 2–3 weeks, with abnormal vision and field of view, and mGCC and pRNFL swelling. The visual field changes and mGCC swelling do not coincide during this period. (3) Mid-term progression and separation period lasted for 2–3 weeks after the onset, with the occurrence of mGCC atrophy, but swollen pRNFL. The vision as well as the visual field was improved when compared with those at the early stage of the disease. The change of visual field in this period was basically consistent with the change of mGCC atrophy. Stabilization and atrophy period showed pRNFL atrophy, which usually lasted for more than 6–8 weeks after the onset. Generally, the disease discontinued to progress and tended to stabilize after 3 months, and then the visual acuity was improved and the visual field was also stabilized. These changes are better than those at the initial stage, but generally do not recover to the original normal levels. At this stage, the change in visual field coincides with changes in mGCC and pRNFL atrophy. Functional changes of ganglion cells (visual field changes) occur (in the early stage) before the organic changes of

the ganglion cells (middle stage). The ganglion cell body showed atrophy first (appeared after 2–3 weeks of onset), and the corresponding ganglion cell axon fiber (mRNFL) also showed atrophy, followed by the atrophy of the pRNFL (6–8 weeks after onset). Generally, the disease becomes stable after 3 months. The time difference between atrophy of ganglion cell bodies and axons (mRNFL, pRNFL) might be related to the fact that the apoptosis of astrocytic-vascular sheath in the periphery of nerve fibers occurs after the atrophy of ganglion cell axons.

The concept and essence of subnormal eye: The latent state of the onset (clinically cured) or the non-onset optic nerve disease or the clinically cured fundus diseases are accompanied by optic nerve damage. Both types of disease had optic nerve damage - mGCC swelling and pRNFL swelling. And the optic disk was stained at the later FFA stage. Therefore, the subnormal eye is essentially considered to be the latent state (most of the cases) or early (very few) manifestation of the eye diseases, which is associated with mGCC swelling and atrophy (fundus diseases, optic neuropathy, and glaucoma). The latent sub-normal eye refers to no clinical symptoms, except for mGCC and pRNFL swelling and stained FFA optic disc during this period, with normal visual acuity and visual field. Therefore, it is considered as the latent period or preclinical period, which may last for long time or for life. Only few cases will have the onset based on this.

The visual field of trans-neuronal descending lesions at the posterior optic tract changes from hours to weeks, and the mGCC atrophy may occur from several months to several years. Nevertheless, the evolution and the characteristics of visual field, mGCC and RNFL in patients with trans-neuronal descending lesions at the posterior optic radiation require further investigation.

## Conclusion

The distribution of ganglion cells is closely related to the visual field. Evaluation of morphological characteristics of the ganglion cells in the macular region of the eyes by SS-OCT can be used to locate the diseases in different parts of the optic pathway-related neuro-ophthalmology.<sup>16-18</sup> The morphological analysis of the ganglion cells remained objective, and has the same value as the subjective positioning diagnosis of the visual field, but is considered to be superior to the visual field inspection. Since mGCC provides only 50% of the neural visual information, accurate visual field examination is still needed to improve the necessary supplement. The authors think that mGCC can not completely replace visual field examination at present, and further research on mGCC is still needed. Meanwhile, the positioning of optic pathway-related neuro-ophthalmologic diseases without changes in mGCC ring in the preclinical or latent stage still should be relied on the visual field and the MRI, and the precise positioning of the optic lesion at the posterior optic chiasm needs the combination of MRI and 90-degree field of view.<sup>19-24</sup> Therefore, applying SS-OCT examination to analyze the morphological changes in mGCC thickness map, and close combination of it with visual field and MRI examination can assist in mutual verification and bring out the best in each other, thus achieving the objective localization value in the diagnosis and treatment of optic pathway-related neuro-ophthalmic diseases.

## Abbreviations

mGCC macular ganglion cell complex SS-OCT swept-source optical coherence tomography pRNFL peripapillary retinal nerve fiber layer LGN lateral geniculate nucleus MRI magnetic resonance imaging FFA fundus fluorescein angiography

## Declarations

## Acknowledgements

Not applicable.

## Funding

No funding was required for the completion of this study.

## Authors' contributions

WZ data collection, data analysis, literature search, manuscript preparation, and manuscript editing. XS conceived of the study. XP data collection, manuscript preparation, manuscript editing, and research supervision. All authors read and approved the final manuscript.

## Ethics approval and consent to participate

Research ethics approval was obtained from Beijing Tongren Eye Hospital Ethics Board. All participants have given written informed consent for the collection and analysis of patient data. Written informed consent was obtained from a parent or guardian for participants under 16 years old.

## Consent for publication

The study received consent for publication as per the research ethics board at the Beijing Tongren Eye Hospital. All of the study patients have agreed with the completion and publication of this study as per the guidelines of the Beijing Tongren Eye Hospital board at the Capital Medical University. All patients described within the study gave informed, written consent for their personal or clinical details along with any identifying images to be published in this study.

## Competing interests

The authors declare that there is no competing interest.

Open Access This article is distributed under the terms of the Creative Commons Attribution 4.0 International License (<http://creativecommons.org/licenses/by/4.0/>), which permits unrestricted use, distribution, and reproduction in any medium, provided you give appropriate credit to the original author(s) and the source, provide a link to the Creative Commons license, and indicate if changes were made. The Creative Commons Public Domain Dedication waiver (<http://creativecommons.org/publicdomain/zero/1.0/>) applies to the data made available in this article, unless otherwise stated.

## References

1. Raza A, Jungsuk C, de Moraes C, et al. Retinal ganglion cell layer thickness and local visual field sensitivity in glaucoma. *Arch Ophthalmol*. 2011;129:1529–1536.
2. Takagi S, Kita Y, Fumihiko Y, Tomita G. Macular retinal ganglion cell complex damage in the apparently normal visual field glaucomatous eyes with hemifield defects. *J Glaucoma*. 2012;21:318–325.
3. Mwanza JC, Durbin M, Budenz D, et al. Glaucoma diagnostic accuracy of ganglion cell-inner plexiform layer thickness: comparison with nerve fiber layer and optic nerve head. *Ophthalmology*. 2012;119:1151–1158.
4. Koh V, Tham YC, Cheung C, et al. Determinants of ganglion cell-inner plexiform layer thickness measured by high-definition optical coherence tomography. *Invest Ophthalmol Vis Sci*. 2012;53:5853–5859.
5. Na JH, Kook M, Lee Y, Baek S. Structure-function relationship of the macular visual field and the ganglion cell complex thickness in glaucoma. *Invest Ophthalmol Vis Sci*. 2012;53:5044–5051.
6. Fisher JB, Jacobs DA, Markowitz CE, et al. Relation of visual function to retinal nerve fiber. *Brain*. 2012;135:521–533.
7. Walter S, Ishikawa H, Galetta K, et al. Ganglion cell loss in relation to visual disability in multiple sclerosis. *Ophthalmology*. 2012;119:1250–1257.
8. Aggarwal D, Tan O, Huang D, Sadun A. Patterns of ganglion cell complex and nerve fiber layer loss in nonarteritic ischemic optic neuropathy by Fourier-domain optical coherence tomography. *Invest Ophthalmol Vis Sci*. 2012;53:4539–4545.
9. Hood D, Raza A, de Moraes C, Liebmann J, Ritch R. Glaucomatous damage of the macula. *Prog Retin Eye Res*. 2013;32:1–21.
10. Kupersmith M, Garvin M, Wang JK, Durbin M, Kardon R. Retinal ganglion cell layer thinning within one month of presentation of optic neuritis. *Mult Scler*. 2016;22:641–648.
11. Gonul S, Koktekir BE, Bakbak B, Gedik S. Comparison of the ganglion cell complex and retinal nerve fibre layer measurements using Fourier domain optical coherence tomography to detect ganglion cell loss in non-arteritic ischaemic optic neuropathy. *Br J Ophthalmol*. 2013;97:1045–1050.

12. Syc S, Saidha S, Newsome S, et al. Optical coherence tomography segmentation reveals ganglion cell layer pathology after optic neuritis. *Brain*. 2012;135:521–533.
13. Green A, McQuaid S, Hauser S, Allen I, Lyness R. Ocular pathology in multiple sclerosis: retinal atrophy and inflammation irrespective of disease duration. *Brain*. 2010;133:1591–1601.
14. Rebolleda G, Sanchez-Sanchez C, Gonzalez-Lopez J, Contreras I, Munoz-Negrete F. Papillomacular bundle and inner retinal thickness correlate with visual acuity in nonarteritic anterior ischemic optic neuropathy. *Invest Ophthalmol Vis Sci*. 2015;56:682–692.
15. Kupersmith, M, Kardon R, Durbin M, Horne MK, Schulman J. Scanning laser polarimetry reveals status of axon integrity in areas of optical coherence tomography revealed thickened
16. retinal nerve fiber layer (RNFL) with optic nerve head swelling. *Invest Ophthalmol Vis Sci*. 2012;53:1962–1970.
17. Kupersmith MJ, Garvin MK, Wang J-K, Durbin M, Kardon R. Retinal ganglion cell layer thinning within one month of presentation for non-arteritic anterior ischemic optic neuropathy. *Invest Ophthalmol Vis Sci*. 2016;57:3588–3593.
18. M. P. Bambó Rubio, E. Garcia-Martin, L. M. Gil-Arribas, et al. Anterior ischaemic optic neuropathy: What do we know and what do we still need to know? *Arch soc esp oftalmol*. 2013;88(3):85–87.
19. Ho JK, Stanford MP, Shariati MA, et al. Optical coherence tomography study of experimental anterior ischemic optic neuropathy and histologic confirmation. *Invest Ophthalmol Vis Sci* 2013;54:5981–5988.
20. Cho JW, Sung KR, Lee S, et al. Relationship between visual field sensitivity and macular ganglion cell complex thickness as measured by spectral-domain optical coherence tomography. *Invest Ophthalmol Vis Sci* 2010;51:6401–6407.
21. Kardon R. The role of the macula OCT scan in neuro-ophthalmology. *J Neuroophthalmol* 2011;31(4):353–361.
22. Shon K, Sung KR. Assessment of macular ganglion cell loss patterns in neurologic lesions that mimic glaucoma. *Korean J Ophthalmol* 2014;28(4):314–322.
23. Gareia Martin E, P010 V, Larrosa JM, et al. Retinal layer segmentation in patients with multiple sclerosis using spectral domain optical coherence tomography. *Ophthalmology* 2014,121(2):573–579.
24. Sung KIL, Wollstein G, Kim NIL, et al. Macular assessment using optical coherence tomography for glaucoma diagnosis. *Br J Ophthalmol* 2012;96(12):1452–1455.
25. Nucci C, Mancino R, Martueci A, et al. 3-T Diffusion tensor imaging of the optic nerve in subjects with glaucoma: correlation with GDx-VCC, HRT-III and Stratus optical coherence tomography findings. *Br J Ophthalmol* 2012;96(7):976–980.

## Table

Table 1

## Baseline patient characteristics

n	gender	age	Vision[R,L]	diagnosis	Visual field change	Atrophy of mGCC ring	Lesion positioning
1	F	58	20/20,20/400	pituitary tumor	Bitemporal hemianopia	Binasal atrophy in mGCC ring based on midperpendicular demarcation	Optic chiasm
2	F	61	20/33,20/25	pituitary tumor	Bitemporal hemianopia	Binasal atrophy in mGCC ring based on midperpendicular demarcation	Optic chiasm
3	F	63	20/25,20/33	Meningioma at posterior junction of the left optic chiasm	Homonymous hemianopia of right side	Nasal atrophy in the right eye and temporal atrophy in the left eye in mGCC ring based on midperpendicular demarcation	Posterior junction of the left optic chiasm
4	M	56	20/800,20/40	craniopharyngioma	Bitemporal hemianopia, right eye crossing midperpendicular line	Bilateral nasal atrophy based on midperpendicular demarcation, right eye crossing the midperpendicular line	Slightly to the right of optic chiasm body
5	M	66	20/800,20/66	pituitary tumor	Bitemporal hemianopia, right eye crossing midperpendicular line	Bilateral nasal atrophy in mGCC ring based on midperpendicular demarcation, right eye crossing the midperpendicular line	Slightly to the right of optic chiasm body
6	M	29	20/25,20/25	pituitary tumor	Bitemporal hemianopia	Bilateral nasal atrophy in mGCC ring based on midperpendicular demarcation	Optic chiasma
7	M	5	20/166,20/25	Dysplasia in optic chiasm-transparent septum deficiency	Bitemporal hemianopia	Bilateral nasal atrophy based on midperpendicular demarcation	Optic chiasma
8	M	32	20/50,20/16	transparent septum deficiency	Temporal hemianopia in the right eye	Nasal atrophy in the right eye in mGCC ring based on midperpendicular demarcation	Slightly to the right of the optic chiasm
9	F	47	20/25,20/20	Hemangioma at starting part of optic tract	Homonymous hemianopia of left side	Nasal atrophy in the left eye and temporal atrophy in the right eye in mGCC ring based on midperpendicular demarcation	Beginning of the right optic tract
10	F	65	20/40,20/33	Ischemic infarction at left occipital lobe	Homonymous hemianopia of right side, macular sparing	Nasal atrophy in the right eye and temporal atrophy in the left eye in mGCC ring based on midperpendicular demarcation, macular sparing	Left occipital lobe (posterior optic radiation or middle of calcarine fissure)
11	M	52	20/20,20/20	Right occipital lobe ischemia	Homonymous hemianopia of left side, macular sparing	Normal mGCC ring-descending transneuron mGCC atrophy has not yet occurred due to short onset time)	Right occipital lobe (posterior optic radiation or middle of calcarine fissure)
12	F	31	20/33,20/25	Tumor at left anterior optic radiation	Bilateral right homonymous hemianopia in upper 1/4 quadrant	Atrophy at lower 1/4 quadrant nasal side in the right eye and lower 1/4 quadrant temporal side in the left eye in mGCC ring based on midperpendicular demarcation	Anterior ring of left optic radiation
13	M	34	20/20,20/20	Ischemia in left posterior optic radiation	Homonymous hemianopia of right side, macular sparing	Nasal atrophy in the right eye, temporal atrophy in the left eye in mGCC ring based on	Posterior segment of left optic radiation or

						midperpendicular demarcation, macular sparing	middle of calcarine fissure
14	M	55	20/20,20/25	Aneurysm in left superior posterior junction of optic chiasm	Homonymous hemianopia of right side	Nasal atrophy in the right eye, temporal atrophy in the left eye which crossed the midperpendicular line in mGCC ring based on midperpendicular demarcation	left superior posterior junction of optic chiasm
15	F	30	20/20,20/25	Left occipital vascular malformationscattered cerebrovascular malformation	Homonymous hemianopia of right side, macular sparing	Nasal atrophy in the right eye, temporal atrophy in the left eye in mGCC ring based on midperpendicular demarcation, macular sparing	Lesion at posterior segment of left optic radiation
16	F	34	20/16,20/20	Right occipital arteriovenous malformation	Homonymous hemianopia of left side retain of left temporal 30-deg crescent	Normal mGCC ring descending transneuron mGCC atrophy has not yet occurred due to short duration after craniotomy)	Middle of calcarine fissure in the right occipital lobe
17	M	40	20/20,20/20	Ischemic infarction at right occipital lobe	Homonymous hemianopia of left side retain of left temporal 30-deg crescent	temporal atrophy in the right eye, nasal atrophy in the left eye in mGCC ring based on midperpendicular demarcation, macular sparing	Middle of calcarine fissure in the right occipital lobe
18	F	61	20/20,20/800	pituitary tumor	Bitemporal hemianopia	Bilateral nasal atrophy in mGCC ring based on midperpendicular demarcation	Optic chiasma
19	F	51	20/400,20/20	pituitary tumor	Blindness in the right eye, temporal hemianopia in the left eye	Complete atrophy in the right eye, nasal atrophy in the left eye in mGCC ring based on midperpendicular demarcation	Slightly to the left of optic chiasm body
20	M	42	20/133,20/33	pituitary tumor	Bitemporal hemianopia, right eye crossing midperpendicular line	Bilateral nasal atrophy in mGCC ring based on midperpendicular demarcation, right eye crossing the midperpendicular line	Slightly to the right of optic chiasm
21	M	77	20/33,20/200	pituitary tumor	Temporal hemianopia in the right eye, and blindness in the left eye	Nasal atrophy in the right eye and complete atrophy in the left eye mGCC ring based on midperpendicular demarcation	Slightly to the left of optic chiasm
22	M	51	20/25,20/20	pituitary tumor	Temporal superior hemianopia in the right eye, temporal hemianopia in the left eye	Bilateral slight nasal atrophy in mGCC ring based on midperpendicular demarcation	Optic chiasma
23	M	24	20/66,20/200	pituitary tumor	Bitemporal hemianopia both extended to nasal side	Bilateral slight nasal atrophy in mGCC ring based on midperpendicular demarcation	Optic chiasma
24	F	18	20/100,20/33	craniopharyngioma	Bitemporal hemianopia, damage in upper nasal quadrant of the right eye	Disappearance of mGCC ring in the right eye, and nasal atrophy in the left eye (based on midperpendicular demarcation)	Right side of optic chiasm
25	M	63	20/20,20/25	Aneurysm in left	Homonymous	Nasal atrophy in the right eye	Left posterior

				posterior junction of optic chiasm	hemianopia of right side	and complete atrophy in the left eye mGCC ring based on midperpendicular demarcation	junction of optic chiasm
26	M	50	20/400,20/25	craniopharyngioma	Bitemporal incomplete hemianopia (midperpendicular demarcation)	Disappearance of mGCC ring in the right eye, nasal incomplete atrophy in the left eye (midperpendicular demarcation)	Right side of optic chiasm
27	F	56	20/200,20/800	pituitary tumor	Bitemporal hemianopia, left eye crossing midperpendicular line	Bilateral mGCC ring swelling, no atrophy(mGCC ring did not occur atrophy in subnormal eye after 1 week of onset)	Slightly to the left of optic chiasm
28	F	73	20/66,20/40	Chordoma or metastatic cancer	Bitemporal hemianopia, right eye crossing midperpendicular line	Bilateral nasal atrophy in mGCC ring based on midperpendicular demarcation, right eye crossing the midperpendicular line	Right side of optic chiasm
29	F	27	20/20,20/20	Pituitary adenoma in the saddle	Normal visual field in both eyes	in bilateral mGCC ring (optic pathway is not involved)	pituitary adenoma in the saddle was located by postoperative MRI
30	F	45	20/25,20/25	Schwannoma beside the right saddle	Irregular reduced visual field sensitivity in the right eye and normal visual field in the left eye	Normal bilateral mGCC ring (optic pathway is not involved)	Beside the right saddle (positioning by MRI)
31	F	58	20/20,20/400	Ischemia optic neuropathy in anterior left eye	Lower hemianopia in the left eye based on horizontal demarcation	Upper atrophy in the left eye in mGCC ring based on horizontal demarcation	Left optic nerve
32	F	52	20/16,20/400	Ischemia optic neuropathy in anterior left eye	Lower hemianopia in the left eye based on horizontal demarcation	Upper atrophy in the left eye in mGCC ring based on horizontal demarcation	Left optic nerve

## Figures

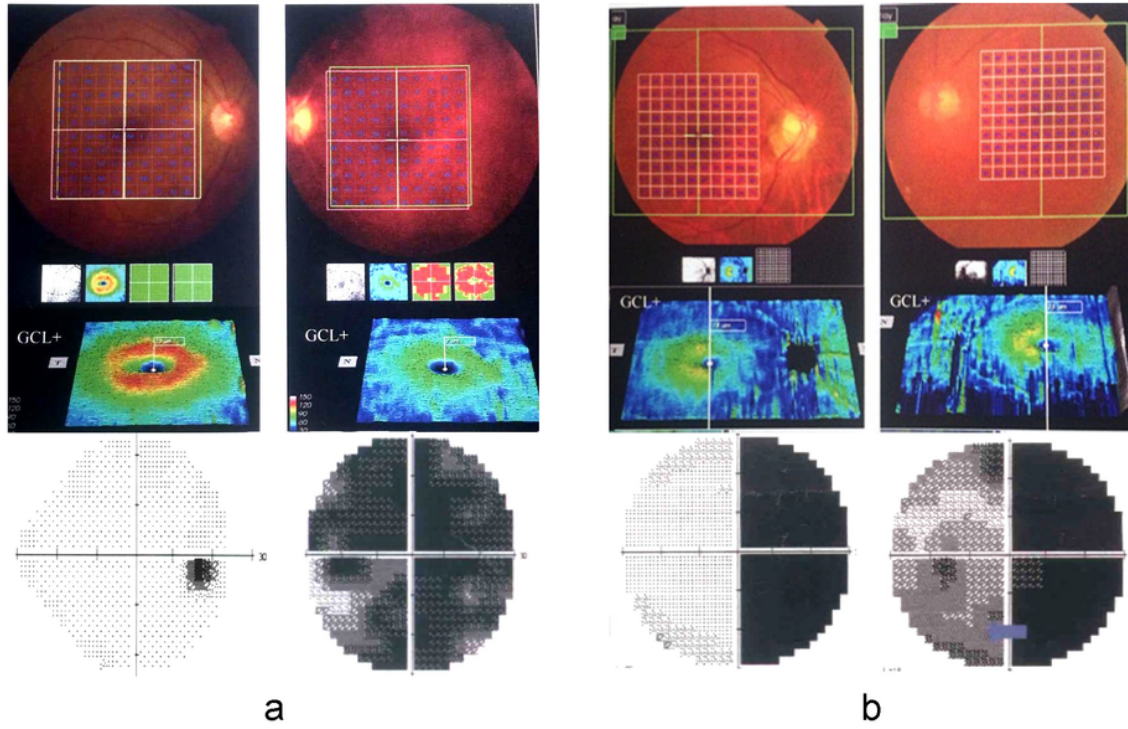


**Figure 1**

a. Left papilloretinitis; b. Ischemia at the posterior segment of the left optic radiation or in the middle of the calcarine fissure.

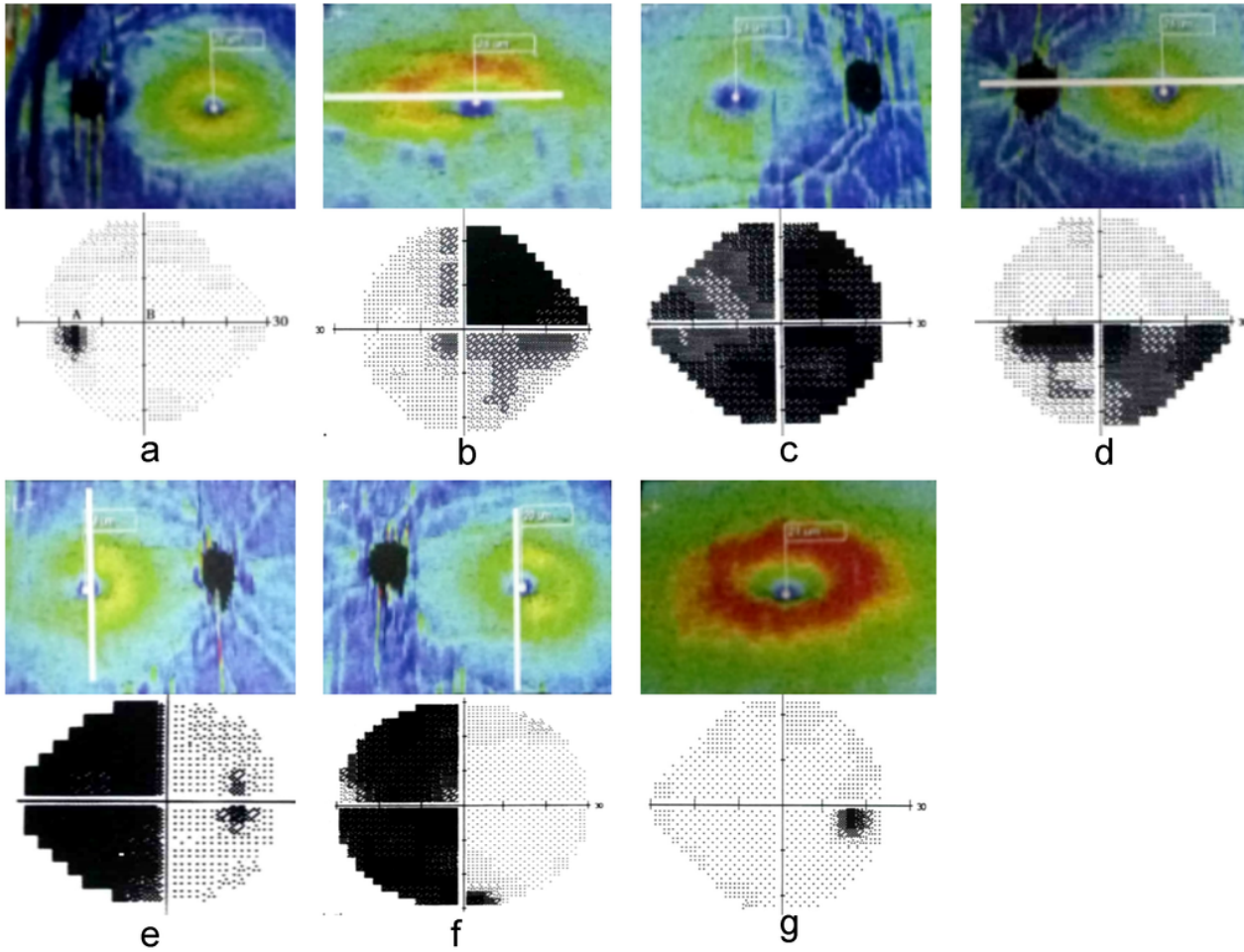


**Figure 2**

a. The normal mGCC ring appeared yellow in shape b-f. Common atrophy forms of mGCC included 1/4 quadrant atrophy, complete atrophy, upper atrophy based on horizontal demarcation, temporal atrophy based on midperpendicular demarcation, nasal atrophy based on midperpendicular demarcation g. Subnormal or swelling period of mGCC appeared red in shape

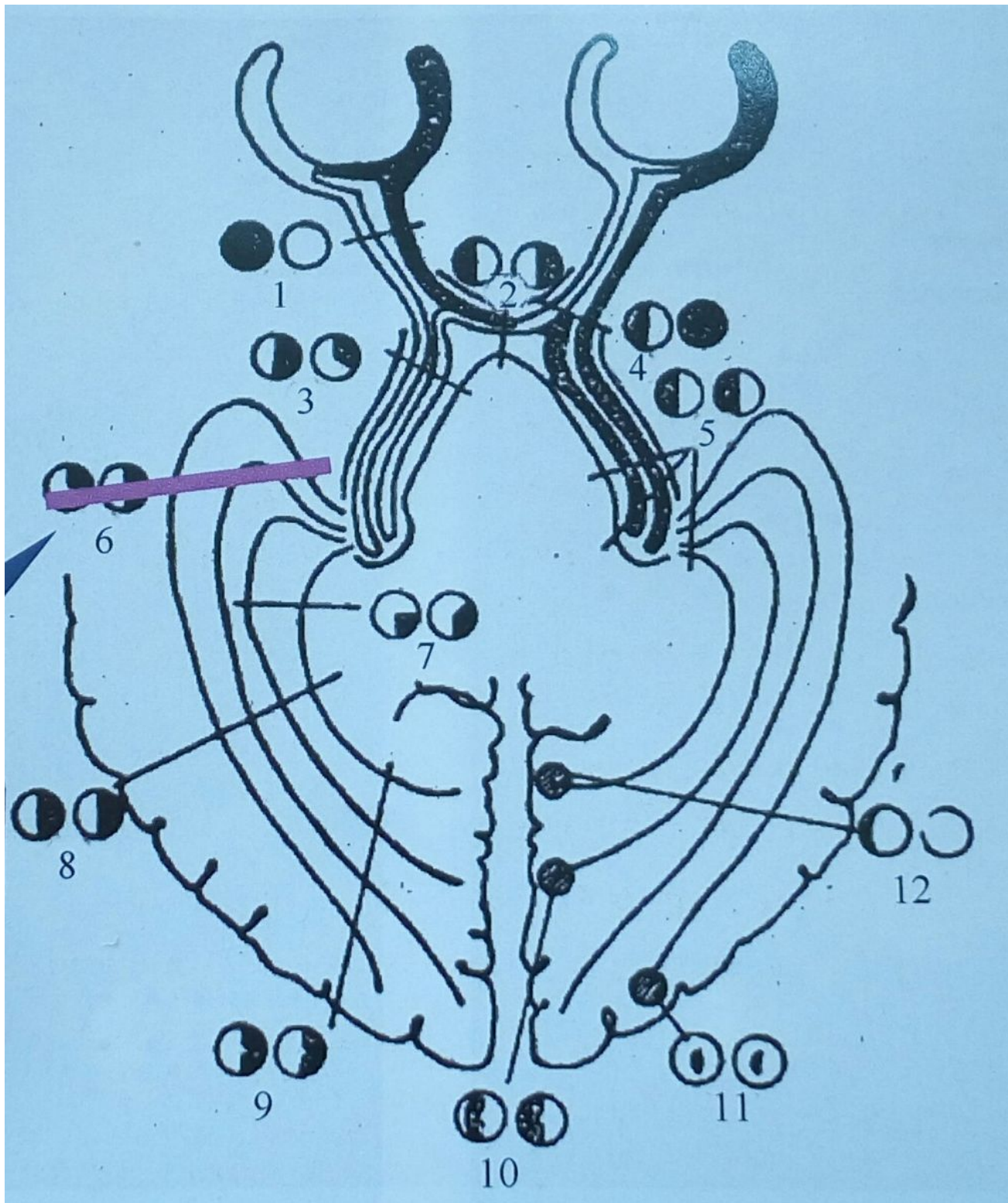


**Figure 3**

Figure 3 1. Optic nerve: blind ipsilateral eye, and normal contralateral eye; 2. Center of optic chiasm: bitemporal hemianopia; 3. Optic tract: asymmetric homonymous hemianopia; 4. Optic nerve junction: ipsilateral blindness, contralateral temporal hemianopia; 5. Posterior segment of optic tract: symmetric homonymous hemianopia; 6. Anterior optic radiation ring: bilateral asymmetric homonymous hemianopia in the upper quadrant; 7. Medial optic radiation: bilateral asymmetric homonymous

hemianopia in the lower quadrant; 8. Optic radiation cross-section: symmetric homonymous hemianopia; 9. Posterior segment of optic radiation: symmetric homonymous hemianopia and macular sparing; 10. Middle of calcarine fissure: symmetric homonymous hemianopia, macular sparing and contralateral crescent sparing; 11. Occipital pole: symmetric homonymous central hemianopia; 12. Anterior calcarine fissure: contralateral crescent defect